Journal of Materials Chemistry B

Accepted Manuscript

ROYAL SOCIETY OF CHEMISTRY

www.rsc.org/materialsB

Inhibition of Glioma Proliferation and Migration by Magnetic Nanoparticle Mediated JAM-2 silencing

Lifeng Qi*[a], Jing Liu[a], Haiyan Zhu[a], Zhuoquan Li[a], Kun Lu[a], Tian Li[a], Donglu Shi*[a,b]

[a]Shanghai East Hospital, The Institute for Biomedical Engineering & Nano Science, Tongji University School of Medicine, Shanghai 200120, China. Email: leonqi168@163.com.

[b]The Materials Science and Engineering Program, Dept. of Mechanical and Materials Engineering, College of Engineering and Applied Science, University of Cincinnati, Cincinnati, Ohio, 45221，USA.

*Supported by Nano 973 Project of China (2010CB933901), NSFC (81371682, 4342234007 and 43422340010), Shanghai Natural Science Foundation (13ZR1443900), Shanghai Nano Project (43422360007), and The Foundation for Innovative Research Groups of the National Natural Science Foundation of China (81221001).

Abstract: Brain invasion is a biological hallmark of glioma that leads to its

aggressiveness and prognosis. Junctional adhesion molecule-2 (JAM-2) was found over-expressed in human glioma. In this study, effects of JAM-2 silencing mediated by cell penetrating magnetic nanoparticles were investigated on glioma cell proliferation and migration in vitro and in vivo. Results showed that deregulation of JAM-2 in glioma cell lines could cause a dramatic decrease in cell proliferation and migration in vitro. The expression level of cytoskeleton remodeling and migration associated protein genes appeared to be a downstream factor of JAM-2. Furthermore, silencing of JAM-2 expression in implanted glioma cells was found to impair in vivo tumor growth significantly. These data provide new evidences for the role of JAM-2 in progression of glioma, and show its great potential in human glioma gene therapeutics.

Key words: JAM-2, glioma, magnetic nanoparticles, siRNA, in vivo.

1. Introduction

As a novel member of the Ig superfamily, junctional adhesion molecule-2 (JAM-2) is a subfamily of junctional adhesion molecules (JAMs) comprising JAM-1 (JAM-A), JAM-2 (JAM-B), and JAM-3 (JAM-C) [1]. JAM-2 is specifically enriched in cell-cell contacts at the level of the tight junction [2], and highly expressed on lymphatic and vascular endothelial cells mostly in high endothelial venules (HEVs) [3,4]. JAM-2 is also expressed on high endothelial venules in human tonsil and on a subset of human leukocytes. JAM-2 plays a central role in regulating transendothelial migration [5,6], the counterligand of JAM-2 was identified as JAM-3 and $\alpha_4\beta_1$, therefore, JAM-2 and JAM-3 are known as the protein-interacting pair that is essential for T, NK, and dendritic cell trafficking and inflammation [7, 8].

JAMs proteins are involved in antitumoral processes. JAM-A was reported to play an important role in driving breast cancer cell migration via activation of Rap 1 GTPase and β1-integrin [9]. JAM-A's over-expression represents a possibility of a new target for reducing breast cancer metastasis，it was shown that abrogation of JAM-A expression can induce breast cancer progression and cell apoptosis [10]. The inactivation of JAM-A was found to enhance antitumoral immune response by promoting dendritic cell and T lymphocyte infiltration [11]. JAM-C was demonstrated to promote metastasis by enhancing the adhesion of fibrosarcoma extracellular matrices and mediating lung carcinoma-endothelial cell interactions [12]. JAM-A and JAM-C were found to be needed for melanoma cell lines transendothelial migration in vitro [13]. JAM-2 was found to be preferentially expressed in the endothelium of arterioles in and around tumors [7]. JAM-2 was also found to be aberrantly expressed in glioma. Monoclonal antibodies blocking JAM-2/3 interaction can impair in vivo glioma growth and invasion [14].

RNA interference is one of the most promising technologies for cancer therapeutics, while the development of a safe and effective small interfering RNA (siRNA) delivery system is still challenging. In our recent study, the silencing of JAM-2 by proton-sponge coated quantum dots was found to inhibit glioma migration in vitro via NOTCH pathway blockage [15]. For in in vivo RNAi studies, more biocompatible gene vector need to be applied. Our recent work reported cell penetrating magnetic nanoparticles for highly efficient siRNA delivery [16]. To further investigate the biological functionality of JAM-2 during glioma progress especially for in vivo studies, JAM-2 siRNA delivery mediated by cell penetrating magnetic nanoparticles was performed in this study. Results showed that JAM-2 silencing could inhibit glioma cell proliferation and migration remarkably. Gene

expression profiles of JAM-2 siRNA transfected glioma cells showed the expression level of cytoskeleton organization and migration-associated protein genes deregulated upon activation of the signal transducer. In vivo JAM-2 siRNA delivery by cell penetrating nanoparticles was found to inhibit growth of implanted glioma cells significantly.

2. Experimental section

Patients' biopsies and cell culture

Biopsies from patients with or without glioma were collected during surgery in Second Affiliated Hospital of Zhejiang University. U251 and U87 glioma cell lines were obtained from cell bank of Chinese Academy of Science. Glioma cells with low JAM-2 expression and non-target control cells were cultured in DMEM (Gibco, US) containing 10% FBS (Gibco, US) and 5 μg/ml puromycin (Gibco, US).

Antibodies

Anti-human JAM-2 mouse monoclonal antibody (H00058494-M01) used for western blotting and IHC was produced by Novus. Anti-human PECAM-1 rabbit monoclonal antibody (ab76533) and Anti-human GAPDH mouse monoclonal antibody (ab37187) used as an isotype control was purchased from Abcam. Goat anti-mouse and goat anti-rabbit biotin used for IHC was purchased from Boster Co. LTD. Goat anti-mouse antibody used for Western blotting was purchased from MultiSciences Biotech Co. LTD (Hangzhou, China).

Western blotting

Glioma cells were lysed in RIPA buffer (50 mM Tris pH 8; 150 mM NaCl; 1% NP40; 0.5% DOC; 0.1% SDS). Twenty micrograms of protein was

electrophoresed using SDS-PAGE (12% poly-acrylamide gel) and transferred to polyvinylidine difluoride (PVDF) membranes (Millipore, US). PVDF membranes were blocked with 5% non-fat milk/1×TBST for 2 hrs. Primary antibodies (JAM-2 used at a dilution of 1:1000, GAPDH used at a dilution of 1:2000) were respectively diluted in 5% non-fat milk/1×TBST. The PVDF membranes were incubated with the antibody mixtures overnight at 4 °C following the manufacturer's instructions. They were then hybridized with anti-mouse secondary antibody (1:1000). Protein bands were visualized using silver film analysis system.

Immunohistochemistry

SABC method was used for investigation of the JAM-2 protein expression. The immunohistochemistry was followed strictly according to the manufacturer's instructions (Boster, Wuhan, China). Briefly, the tissue slices were incubated in 3% H_2O_2 and blocked with 5% BSA. They were sequentially incubated with the anti-JAM-2 antibody (1:200), biotin-conjugated second antibody (1:1000), and SABC. For cryosections, tumor tissues were inflated with OCT before embedding. 7μm tissue was fixed in methanol (5 min, 220°C), dried, and rehydrated in PBS with 0.5% BSA before processing for immunostaining.

Preparation of cell penetrating magnetic nanoparticles for siRNA delivery

Cell penetrating magnetic nanoparticles were prepared according to our recent work [16]. Briefly, PMAL amphipol was used to transfer hydrophobic magnetic nanoparticles (Nanomics Biopharm, Wuxi, China) to water-soluble nanoparticles. PMAL-modified magnetic nanoparticles were conjugated with protamine peptide by standard EDC-NHS chemistry, then purified by dialysis membrane to remove

unreacted peptide. The purified and sterilized nanoparticles were stored at 4 ℃ for direct use. The morphology and particle size of cell penetrating magnetic nanoparticle was characterized by TEM and zeta sizer respectively. The binding capacity of cell penetrating magnetic nanoparticles with siRNA was studied by 0.8% agarose gel electrophoresis.

JAM-2-targeting sequence of siRNA was CCGGGCTCCTGAATACACATGGTTTCTCGAGAAACCATGTGTATTCAGGAG CTTTTTG. As an isotype control, a non-target siRNA (Sigma, US) was also transduced respectively into U251 and U87MG cells. The JAM-2 targeting and control siRNA were labeled with FITC on sense strand. In the following experiments, U87MG-1 and U251-1 cells were named as U87MG and U251 cells respectively transfected with targeted JAM-2 siRNA, while U87MG-2 and U251-2 cells were named as those control cells transfected with scrampled JAM-2 siRNA.

RNA expression analysis

The total RNA of the glioma sample was extracted with RNAiso™ Plus (TaKaRa, Japan). RNA was treated with RNase-free DNase I (TaKaRa, Japan) for 45 min according to the manufacturer’s protocols. The final amount of purified RNA was quantified by ultraviolet spectrophotometer. Total RNA (1μg) was reverse-transcribed using the SYBR PrimeScript RT-PCR kit II (TaKaRa, Japan) with random hexamer priming method according to the manufacturer's recommendations. The following are the sequences of the oligonucleotides used, JAM-2: F=TCTTCTTTGGGGTTTTGCAG, R=TACCTGGTGGTCGCCCT, GAPDH: F=TGAGGCCGGTGCTGAGTATGTCGTG, R=TCCTTGGAGGCCATGTAGGCCAT.

Cell proliferation and migration assays

Cell proliferation was assayed using a 3-(4,5-dimethylthiazol-2-yl)-2,5-diphenyltetrazolium bromide (MTT) staining kit (Sigma-Aldrich, US) according to the manufacturer's protocol. The glioma cells were grown in 96-well plates for six days. The MTT absorbance data was taken at 490 nm by ultraviolet spectrophotometer.

Cell migration assay was performed using transwell chambers (6.5 mm diameter; 8 μm pore size polycarbonate membrane) obtained from Corning. 2 x 10^5 cells in 0.2 ml FBS-free DMEM were loaded in the upper chamber, whereas the lower chamber was placed with 0.5 ml medium containing 15% FBS. After 48 hours' incubation, the total number of cells that migrated into the lower chamber was counted under an inverted light microscope (Axiovert 25, Carl Zeiss AG, Gottingen, Germany, equipped with an Olympus SC 35 Camera, Volketswil, Switzerland) at ×400.

In vivo tumor growth

In order to study the silencing effects of JAM-2 by cell penetrating magnetic nanoparticles, U87MG cells stably transfected with an eGFP by lentiviral particles carrying a gene encoding for eGFP plasmid and a puromycin resistance (Sigma-Aldrich, US) were established. At day 0, female inbred BALB/c mice (aged 6-8 weeks) were subcutaneously (s.c.) inoculated into the flank respectively with the U87MG-eGFP cells (3 x 10^5/0.1 ml). After inoculation, mice were randomized into 3 groups (each with n = 5). Cell penetrating magnetic

nanoparticles mixed with JAM-2 targeting and control siRNA respectively, then injected by intravenous administration through mice tail vein. In vivo transfected mice were scored for tumor growth once every five days by measuring the diameters of the s.c. tumors and weight loss with a Vernier caliper. Animals were euthanized 6 weeks post-operatively by transcardial perfusion using 4% paraformaldehyde. Mouse tumor and lung tissues were harvested, fixed in 4% paraformaldehyde overnight at 4 °C, and transferred into 30% sucrose. Tissues were paraffin-embedded and sectioned for hemotoxylin and eosin staining. At the end of the experiment, tumors were excised to validate the antitumor effects. Mice were maintained under guidelines that are established in the guide for Care and Use of Laboratory Animals (NIH publications, 1986).

Statistical analysis

Results are expressed as mean ± standard deviation. Significance of difference was calculated by Student's t test or Mann Whitney. All experiments were performed by triplicate and repeated at least three times, with comparable results.

3. Results and discussion

JAMs are a family of glycoproteins characterized by two immunoglobulin folds (VH- and C2-type) in the extracellular domain [1]. As one subfamily of JAMs, JAM-2 has a more restricted distribution mostly in high endothelia venules (HEVs), which are portals of entry into lymphatic tissues for lymphocytes responding to processed antigens [4]. Over-expression of JAM-2 was observed in glioblastoma within the normal brain [14]. In a recent study of ours, silencing of JAM-2 in glioma cells was found to inhibit glioma migration significantly by

blockage of the NOTCH1 pathway [15]. The in vitro and vivo study of JAM-2 in glioma was carried out to investigate the underlying signal transducer events, and the effects of stable JAM-2 siRNA transfection in glioma cells on cell growth, invasion, mRNA expression profile, and in vivo tumor growth.

In order to study the function of JAM-2 in glioma cells, U251 and U87MG cells were transfected with JAM-2 targeted siRNA and a scrambled siRNA respectively. The prepared cell penetrating magnetic nanoparticles were characterized by TEM image and particle size. The binding capacity of cell penetrating nanoparticles with siRNA was examined by 0.8% agarose electrophoresis. As shown in Figure 1, the cell penetrating magnetic nanoparticles exhibited uniform morphology and with particle size about 15 nm. The gel mobility of cell penetrating nanoparticles was enhanced greatly compared with control magnetic nanoparticles without peptide modification. Cell penetrating magnetic nanoparticles demonstrated high affinity with siRNA molecules up to higher than 1:20 molar ratio.

RT-PCR and Western blot were used to confirm the knockdown efficiency of the siRNA transfection. As shown in Figure 2, compared with control cells without any treatment and with non-targeting siRNA sequence delivery, JAM-2 expression is downregulated to 30% at both mRNA and protein level in U251-1 cells, while that is almost completely silenced in U87MG-1 cells upon JAM-2 siRNA delivery.

Cell proliferation assays were performed to determine the effects of JAM-2 knockdown on glioma cells growth. Glioma cells were transfected with JAM-2 target and control siRNA respectively. As shown in Figure 3, significant difference is observed on cell growth among three groups from the 72 h's culture. On the

sixth day of culture, glioma cell growth of U87MG-1 and U251-1 cells with low JAM-2 expression was retarded about 95% and 86% respectively compared with the non-targeted control cells (Figure 3A). Fluorescence microscope imaging showed the intracellular JAM-2 siRNA delivery by cell penetrating magnetic nanoparticles, as shown in Figure 3B.

Cell penetrating magnetic nanoparticles for siRNA delivery have been developed by our group recently, where the magnetic nanoparticles were modified with protamine, one kind of arginine-rich cell penetrating peptide (CPPs) [16]. In recent years, arginine-rich CPPs, that are relatively short cationic and/or amphipathic peptides, have received great attention as efficient cellular gene delivery vectors due to their intrinsic ability to enter cells and mediate uptake of plasmid DNA (pDNA), small interfering RNA (siRNAs), and nanoparticulate pharmaceutical carriers [17-19]. L-arginine modified polymer have been demonstrated as efficient non-viral gene delivery vectors while with little cytotoxicity [20]. The enhanced siRNA intracellular delivery by cell penetrating magnetic nanoparticles is attributed to their excellent endosomal escape of nanoparticles-siRNA complexes due to the CPPs' modification.

JAM-2 was mostly over-expressed in U251 cells, reported in our previous study [15]. Using the RNA interference (RNAi) technique, we obtained the U251-1 and U87MG-1 cells with reduced levels of JAM-2 protein compared with the U251-2 and U87MG-2 cells transfected with scrambled JAM-2 siRNA. These two kinds of transfected cell lines were then used for the comparative gene expression analysis. In the JAM-2 silencing U251-1 and U87MG-1 cells, respectively with 18.5-fold and 14.6-fold JAM-2 deregulation showed by affymetrix microarray analysis, 14 genes down and 5 genes up-regulated (Table 1)

were founded. Among the differentially expressed genes, several are known to be involved in cytoskeleton reorganization, cell migration, and invasion. The Actin binding associated genes, such as SPTBN5, TAGLN, DIXDC1, APIRE2, BAIAP2L1 and DMD were deregulated significantly after JAM-2 knockdown. Among them, DMD (differentially methylated domains) was the most differentially expressed gene with a 5.88-fold and 6.57-fold decrease respectively in U251-1 and U87MG-1 cells. The structural molecule activity related genes, such as KRT6B, PLP1, AP4E1, KRT25 and TTC23 were also deregulated and correlated with JAM-2 deregulation. The cytoskeleton reorganization associated genes were the downstream factor of JAM-2. On the other hand, the signal transducer activities of glioma cells, with low JAM-2 expression, were activated to inhibit tumor cell growth and maintenance. TFG, RGS7, GNG2 and TICAM1 were up-regulated significantly. TFG (TRR-fused gene) has been identified as a novel member of the NF-kappaB pathway [21]. It was found in this study to be mostly up-regulated with an 8.4-fold and 11.2-fold increase respectively in U251-1 and U87MG-1 cells. RGS7 and GNG2 were G-protein coupled receptor protein signaling pathways. TICAM1 gene expression indicated macrophage activation during immune response. PVR, a receptor activity related gene, which was implicated in glioma invasion [22], was deregulated with JAM-2 expression in glioma cells.

The correlation between expression of JAM-2 and genes was investigated in terms of cytoskeleton dynamics and cell motility. In vitro cell migration assays were performed by comparing the counterparts of U251-1 vs. U251-2 cells, and the U87MG-1 vs. U87MG-2 cells. Cell migration was studied by use of transwells chambers. As shown in Figure 4, after JAM-2 knockdown, glioma cell migration is inhibited significantly compared with control cells without any treatment. An average reduction of 87% and 82% ($p<0.01$) in cell migration was observed

respectively in U87MG-1 and U251-1 cells with low JAM-2 expression.

The effects of JAM-2 knockdown on a subcutaneous U87MG xenograft model was studied by U87MG cells implanted mice, cell penetrating magnetic nanoparticles complexed with JAM-2 siRNA and scrambled siRNA were intravenous administrated respectively, followed by 6 weeks' growth. Tumor size diameters were measured every five days to determine the effects on tumor growth. JAM-2 knockdown inhibited xenograft growth up to 95%, compared with the scrambled siRNA control, while no significant on body weight increase (Figure 5). Upon dissection, the tumor size of control group was found to be much larger than those of the JAM-2 siRNA targeted group. Only two in five mice from JAM-2 silencing group showed macroscopical tumor tissues, with one displayed GFP expression, indicating the presence of tumor cells (Figure 6A). Histologically, scrambled siRNA tumors exhibited large, distinct areas of tumor formation (Figure 6B), whereas the JAM-2 siRNA expressing xenografts were much smaller and exhibited tumor necrosis morphology, and showed decreased JAM-2 and PECAM-1 expression. These data are clear evidences of JAM-2 expression being required for the in vivo growth of glioma cells.

Gene profile experiments were carried out on the mRNA prolife of U251-1 and U87MG-1 cells after JAM-2 silencing. Results showed that deregulation of the cytoskeleton reorganization associated genes were correlated with JAM-2 silencing. The signal transducer activities of glioma cells, with low JAM-2 expression, are activated to inhibit tumor cell growth and maintenance. DMD (differentially methylated domains) is the most differentially expressed gene in JAM-2 suppressed cells. DMD located between IGF2 and H19 on human chromosome 11 has been found to regulate insulin-like growth factor 2 (IGF2) gene imprinting [23]. The loss of IGF2 imprinting is responsible for tumor growth

inhibition in vitro and in vivo [24]. KRT6B and PLP1 are significantly deregulated in JAM-2 low expression glioma cells. KRT6B is known as a gene with cell growth and maintenance activity [25]. PLP1, a signature gene specific to oligodendrocytes, is always expressed in glioblastoma with high oligodendroglioma [26]. The deregulation of PLP1 showed the decreased malignant grade of glioma cells with low JAM-2 expression. PVR, associated with interspecies interaction between organisms, is regarded as a functional link with glioma invasion [27]. Deregulated PVR expression in glioma cells with low JAM-2 expression indicates a reduced cell invasion capacity.

RGS7 and GNG2 are G-protein coupled receptor protein signaling pathway related gene, they are upregulated greatly upon deregulation of JAM-2. TFG (TRR-fused gene) is a novel member of NF-kappaB pathway, TFG protein has been found to enhance the tumor necrosis factor (TNF)-α, TANK, TNF receptor-associated TRAF2 and TRAF6 by inducing the NF-kappaB activity [28]. On the other hand, (TNF)-α is known to prevent the proteasome-dependent degradation of RGS7, a regulator of G-protein signaling [29]. (TNF)-α has also been reported to induce NF-κB activation in GBM [30]. GNG2, a G-protein signaling pathway associated gene, is shown to be upregulated in glioma cells with JAM-2 silencing. Increased protein expression level of GNG2 alone can inhibit proliferation of malignant tumor cells in vitro and in vivo. These data suggests that JAM-2 could be a novel molecular target for malignant tumor therapy [31].

4. Conclusion

In summary, our experimental results have shown significant inhibition of the cell growth, cell migration and invasion by deregulated JAM-2 expression in glioma cells. In vivo growth of implanted glioma was also inhibited significantly by JAM-2 silencing mediated by cell penetrating magnetic nanoparticles. Cytoskeleton reorganization associated genes are deregulated in correlation to JAM-2 silencing that disrupts cell maintenance and invasion. Insulin-like growth factor 2 gene (IGF2) imprinting has been successfully suppressed. The TFG and TNF-alpha mediated NF-kappaB pathway and G-protein signaling have been activated to inhibit glioma proliferation.

Conflict of interest

The authors declare no conflict of interest.

REFERENCES

[1] G. Bazzoni, *Curr. Opin. Cell Biol.,* 2003, **15**, 525.

[2] I. Martin-Padura, S. Lostaglio, M. Schneemann, L. Williams, M. Romano, P. Fruscella, C. Panzeri, A. Stoppacciaro, L. Ruco, A. Villa, D. Simmons, E. Dejana, *J. Cell. Biol*., 1998, **142**, 117.

[3] M. Aurrand-Lions, C. Johnson-Leger, C. Wong, L. Du Pasquier, B.A. Imhof. *Blood,* 2001,**98**,3699.

[4] D. Palmeri, A. Van Zante, C-C, Huang, S. Hemmerich, S.D. Rosen, *J. Biol. Chem.,* 2000, **275**, 19139.

[5] C.A. Johnson-Léger, M. Aurrand-Lions, N. Beltraminelli, N. Fasel, B.A. Imhof, *Blood,* 2002, **100**, 2479.

[6] M.A. Aurrand-Lions, L, Duncan, C. Ballestrem, B.A. Imhof, *J. Biol. Chem*., 2001, **276**, 2733.

[7] T.W. Liang, H.H. Chiu, A. Gurney, A. Sidle, D.B. Tumas, P. Schow, J. Foster, T. Klassen, K. Dennis, R.A. DeMarco, T. Pham, G. Frantz, S. Fong, *J. Immunol.,* 2002, **168**, 1618.

[8] S.A. Cunningham, J.M. Rodriguez, M.P. Arrate, T.M. Tran, T.A. Brock, *J. Biol. Chem.,* 2002, **277**, 27589.

[9] E.A. McSherry, K. Brennan, L. Hudson, A.D. Hill, A.M. Hopkins, *Breast Cancer Res.,* 2011, **13**, R31.

[10] M. Murakami, C. Giampietro, M. Giannotta, M. Corada, I. Torselli, F. Orsenigo, A. Cocito, G. d'Ario, G. Mazzarol, S. Confalonieri, P.P. Di Fiore, E. Dejana, *PLoS One,* 2011, **6**, e21242.

[11] M. Murakami, C. Francavilla, I. Torselli, M. Corada, L. Maddaluno, A. Sica, G., Matteoli, I.D. Iliev, A. Mantovani, M. Rescigno, U. Cavallaro, E. Dejana, *Cancer Res.,* 2010, **70**, 1759.

[12] H.F. Langer, V.V. Orlova, C. Xie, S. Kaul, D. Schneider, A.S. Lonsdorf, M. Fahrleitner, E.Y. Choi, V. Dutoit, M. Pellegrini, S. Grossklaus, P.P. Nawroth, G. Baretton, S. Santoso, S.T. Hwang, B. Arnold, T. Chavakis, *Cancer Res.,* 2011, **71**, 4096.

[13] S. Ghislin, D. Obino, S. Middendorp, N. Boggetto, C, Alcaide-Loridan, F. Deshayes, *Pigment Cell Melanoma Res.,* 2011, **24**, 504.

[14] M. Tenan, M. Aurrand-Lions, V. Widmer, A. Alimenti, K. Burkhardt, F. Lazeyras, M.C. Belkouch, P. Hammel, P.R. Walker, M.A. Duchosal, B.A. Imhof, P.Y. Dietrich, *Glia,* 2010, **58**, 524.

[15] L. Qi, W. Shao, D. Shi, *J. Mater. Chem. B,* 2013, **1**, 654.

[16] L. Qi, L. Wu, S. Zheng, Y. Wang, H. Fu, D. Cu, *Biomacromolecules,* 2012, **13**, 2723.

[17] S.M. Farkhani , A. Valizadeh, H. Karami, S. Mohammadi, N. Sohrabi, F. Badrzadeh, *Peptides*, 2014, **57**, 78-94.

[18] Y. Chen, P. Xu, M. Wu, Q. Meng, H. Chen, Z. Shu, J. Wang, L. Zhang, Y. Li, J. Shi, *Adv. Mater.* 2014, **26**, 4294-301.

[19] Y. Chen, P. Xu, H. Chen, Y. Li, W. Bu, Z. Shu, Y. Li, J. Zhang, L. Zhang, L. Pan, X. Cui, Z. Hua, J. Wang, L. Zhang, J. Shi, *Adv. Mater*. 2013, **25**, 3100-3105.

[20] J. Wu, D. Yamanouchi, B. Liu, C. Chu, *J. Mater. Chem*. 2012, **22,** 18983-18991.

[21] C. Miranda, E. Roccato, G. Raho, S. Pagliardini, M.A. Pierotti, A. Grec, *J. Cell Physiol.,* 2006, **208**, 154.

[22] K.E. Sloan, J.K. Stewart, A.F. Treloar, R.T. Matthews, D.G. Jay, *Cancer Res*., 2005, **1**, 10930.

[23] D. Astuti, F. Latif, K. Wagner, D. Gentle, W.N. Cooper, D. Catchpoole, R. Grundy, A.C. Ferguson-Smith, E.R. Maher, *Br. J. Cancer,* 2005, **25**, 1574.

[24] Y. Pan, B. He, Z. Lirong, Z. Nie, L. Chen, L. Gu, A.R. Hoffman, S. Wang, J. Hu, *Oncol. Rep.,* 2013, **30**, 1814.

[25] J.C. Lessard, S. Piña-Paz, J.D. Rotty, R.P. Hickerson, R.L. Kaspar, A. Balmain, P.A. Coulombe, *Proc. Natl. Acad. Sci. U S A*, 2013, **110**, 19537.

[26] J. Kong, L.A. Cooper, F. Wang, J. Gao, G. Teodoro, L. Scarpace, T. Mikkelsen, M.J. Schniederjan, C.S. Moreno, J.H. Saltz, D.J. Brat, *PLoS One*, 2013, **8**, e81049.

[27] K.E. Sloan, J.K. Stewart, A.F. Treloar, R.T. Matthe ws, D.G. Jay, *Cancer Res*., 2005, **65**, 10930.

[28] C. Miranda, E. Roccato, G. Raho, S. Pagliardini, M.A. Pierotti, A. Greco. *J, Cell Physiol*., 2006,**208**,154.

[29] T. Benzing, M. Köttgen, M. Johnson, B. Schermer, H. Zentgraf, G. Walz, E.

Kim, *J. Biol. Chem.*, 2002, **277**,32954.

[30] B.C. McFarland, S.W. Hong, R. Rajbhandari R, G.B. Twitty Jr, G.K. Gray, H. Yu, E.N. Benveniste, S.E. Nozell, *PLoS One,* 2013, **8**, e78728.

[31] I. Yajima, M.Y. Kumasaka, H. Tamura, N. Ohgami, M. Kato, *J. Dermatol. Sci.*, 2012, **68**,172.

Table 1. Genes differentially expressed in JAM2 knockdown Cells (U87MG-1, U251-1) compared with U87MG-2 and U251-2 cells

Gene Symbol	Gene Ontology Biological Process	Gene Ontology Molecular Function	Fold (U87MG-1)	Fold (U251-1)	Reg
SPTBN5	actin cytoskeleton organization	actin binding	4.25	3.07	down
TAGLN	muscle organ development	actin binding	3.17	2.88	down
DIXDC1	multicellular organismal development	actin binding	3.69	2.56	down
SPIRE2	transport	actin binding	3.58	2.24	down
SHROOM 1	cell morphogenesis	actin binding	2.69	2.05	up
BAIAP2L1	signal transduction	actin binding cytoskeletal adaptor activity	2.78	2.01	down
DMD	cytoskeletal anchoring at plasma membrane	actin binding	6.57	5.88	down
KRT6B	ectoderm development	structural constituent of cytoskeleton	5.34	4.15	down
PLP1	integrin-mediated signaling pathway myelination in the central nervous system	structural molecule activity	4.72	3.80	down
AP4E1	intracellular protein transport vesicle-mediated transport	structural molecule activity	3.25	2.64	down
KRT25	hair follicle morphogenesis Intermediate filament organization	structural molecule activity	3.61	2.15	down
KRT6B	ectoderm development	structural molecule	5.34	4.15	down
TTC23	intermediate filament cytoskeleton organization	structural molecule activity	5.62	4.00	down
TFG	positive regulation of I-kappaB Kinase NF-kappaB cascade	signal transducer activity	11.25	8.40	up
RGS7	G-protein coupled receptor protein signaling pathway	signal transducer activity	4.67	3.56	up
TICAM1	macrophage activation during immune response	signal transducer activity	3.59	2.27	up
GNG4	signal transduction //regulation	signal transducer	3.15	2.26	down

Gene Symbol	Gene Ontology Biological Process	Gene Ontology Molecular Function	Fold (U87MG-1)	Fold (U251-1)	Reg
	of G-protein coupled receptor Protein signalingpathway hormone-mediated signaling negative regulation of cell growth	activity			
GNG2	G-protein coupled receptor protein signaling pathway cell proliferation // hormone-mediated signaling	signal transducer activity	3.51	2.19	up
PVR	interspecies interaction between organisms	receptor activity	4.12	2.39	down
JAM2	cell-cell adhesion		18.5	14.6	down

Figure Captions

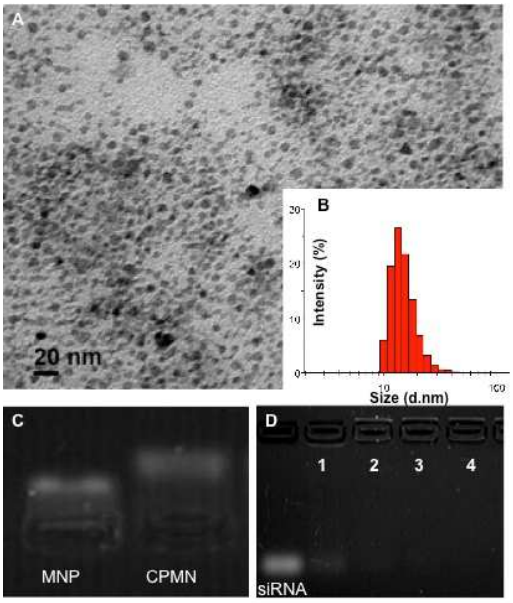

Figure 1. TEM photograph (A) and particle size (B) of cell penetrating magnetic nanoparticles (CPMN); C: Gel mobility of magnetic nanoparticles (MNP) and CPMN; D: siRNA binding affinity of CPMN at different molar ratio versus siRNA as 1:30 (lane 1), 1:20 (lane 2), 1:10 (lane 3) and 1:5 (lane 4);

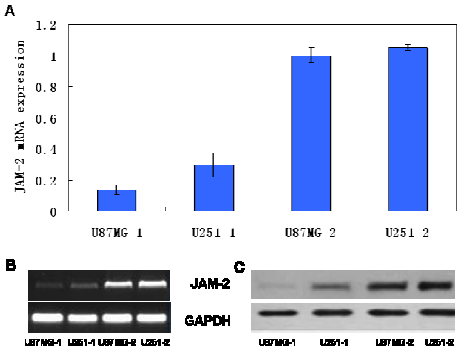

Figure 2. JAM-2 expression in U251 and U87MG glioma cells after JAM-2 targeted siRNA transfection by cell penetrating magnetic nanoparticles, A: relatively quantified JAM-2 mRNA expression by RT-PCR in U87MG-1, U251-1, U87MG-2 and U251-2 cells and their agrose gel image (B). U87MG-1 and U251-1 cells were derived respectively from U87MG and U251 cells transducted with targeted JAM-2 siRNA, while U87MG-2 and U251-2 cells were derived from those with scrampled JAM-2 siRNA; C: Corresponding western blot results of JAM-2 protein expression in U87MG-1, U87MG-2, U251-1 and U251-2 cells. GAPDH expression is used as an isotype control.

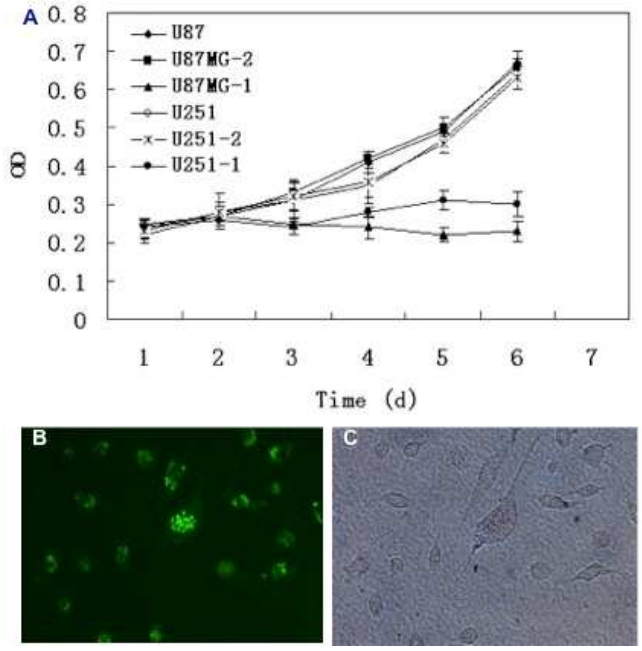

Figure 3. Cell proliferation assays on U87MG and U251 glioma cell lines in 6 days by MTT method. U87MG-1 and U251-1 cells were derived respectively from U87MG and U251 cells transducted with targeted JAM-2 siRNA, while U87MG-2 and U251-2 cells were derived from those with scrampled JAM-2 siRNA, the proliferation of U87MG and U251 cells with JAM-2 low expression is highly inhibited during six culture days. Fluorescent image (B) and corresponding bright field image (C) of intracellular JAM-2 FITC labeled siRNA delivery via CPMN into U87MG cells.

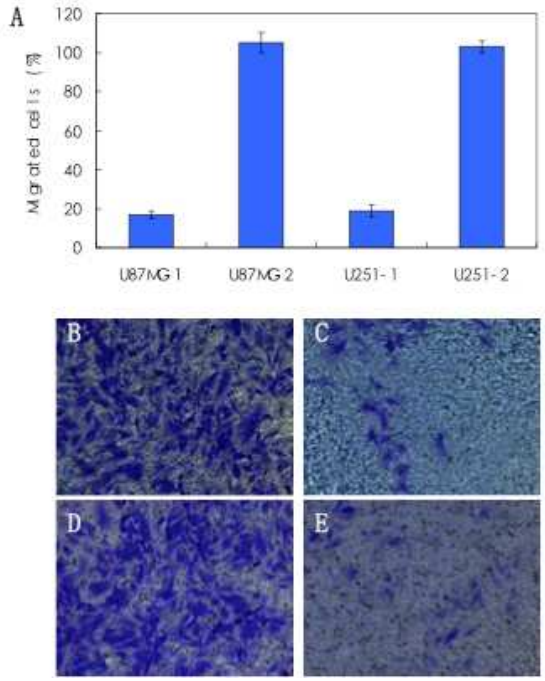

Figure 4. Cell migration assays with transwells. After 48 hours' incubation, the total number of cells that have migrated into the lower chamber is counted (A), and the corresponding photos are taken under a light microscope at ×400, B: U87MG cells with target JAM-2 delivery; C: U87MG-2 cells with control JAM-2 siRNA delivery; D: U251-1 cells with target JAM-2 delivery; E: U251-2 cells with control JAM-2 siRNA delivery.

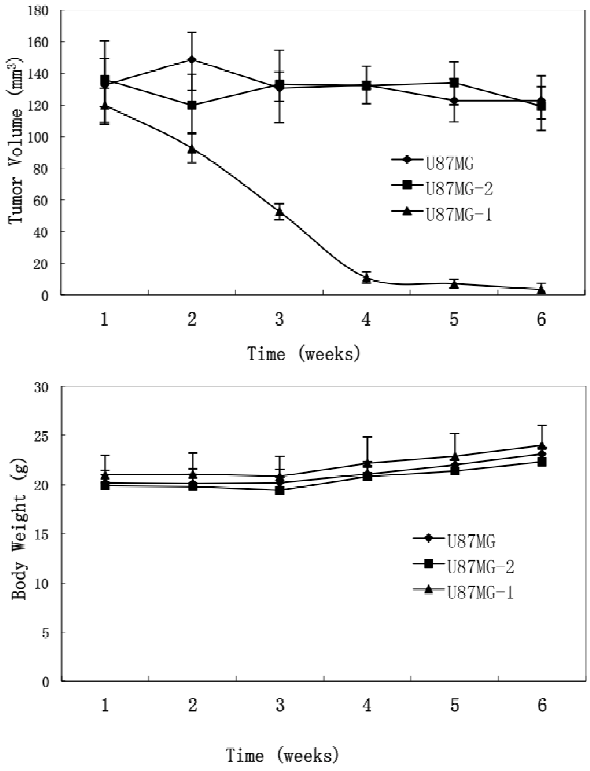

Figure 5. JAM-2 knockdown in U87MG cells inhibits in vivo glioma growth, the figure is referred to the tumor volume analysis, and the body weight increase during the 42 days mice growth, post tumor cell implantation, and the values obtained from five mice treated with control U87MG cells and U87MG-1 cells after JAM-2 siRNA delivery and U87MG-2 after scrambled JAM-2 siRNA delivery.

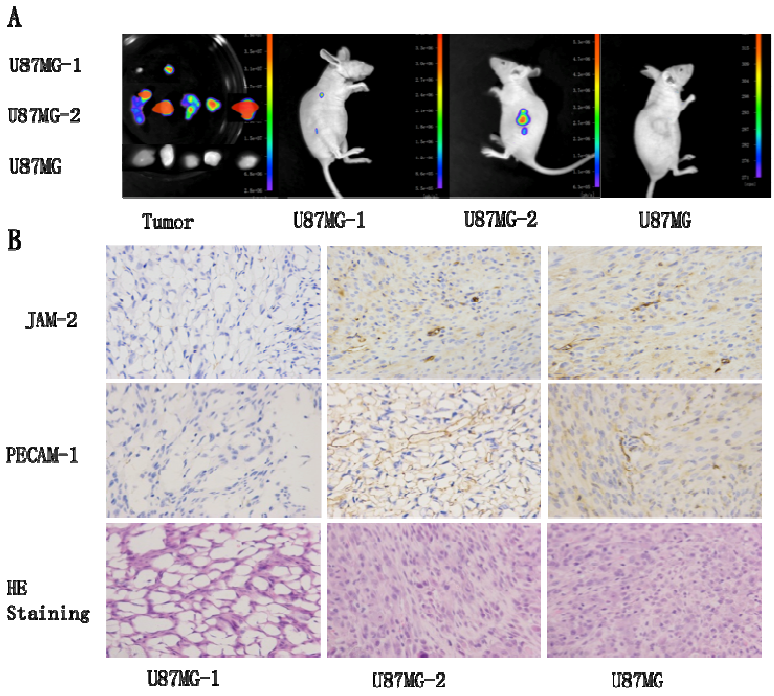

Figure 6. The macroscopic appearance of excised tumor and nude mice from different groups under In vivo animal fluorescence imaging instrument (A) and representative pictures of haematoxylin/eosin staining of tumor sections used for quantification of JAM-2, PECAM-1 expression and cell morphology observation (B). The tumor tissues and sections were obtained from five mice treated with control U87MG cells and U87MG-1 cells after JAM-2 siRNA delivery and U87MG-2 after scrambled JAM-2 siRNA delivery.